metals

MDPI

Article

The Experimental and Theoretical Studies on Corrosion Phenomena of a Welded Stainless-Steel Pipe Under Salt Vapor Conditions

Trinet Yingsamphancharoen [1,3], Chootrakul Siripaiboon [2], Aphichart Rodchanarowan [1,*]

[1] Department of Materials Engineering, Faculty of Engineering, Kasetsart University, 50 Ngamwongwan Rd., Ladyao, Chatuchak, Bangkok 10900, Thailand; trinet2518@hotmail.com
[2] Department of Mechanical Engineering, Faculty of Engineering, Siam University,38 Petchkasem Road, Bang Wa, Phasi Chareon, Bangkok 10160, Thailand;
[3] Center ofWelding Engineering and Metallurgical Inspection, Science and Technology Research Institute, King Mongkut's University of Technology North Bangkok, 1518, Pracharat 1 Road, Wongsawang, Bangsue, Bangkok 10800, Thailand;
* Correspondence: fengacrw@ku.ac.th; Tel.: +662-797-0999 (ext. 2102-4)

Abstract: This work studied the corrosion of welded pipes and how welding destroyed surface film of pipes. Surface reaction of a welded pipe is key to understanding phenomena and important factors during the corrosion. This paper presents experiment and CFD modeling approaches of a welded pipe corrosion under salt vapor condition. The pipes were welded at currents of 60 A,70 A and 80 A to observe the effect of welding current on corrosion. A welded pipe is a stainless-steel ASTM A312 grade 304L and period of experiment about 0-600 hours that they are tested in vertical and horizontal alignments. In CFD software, there is not direct model of corrosion but it can use surface reaction and create add-on species and chemical reaction technique for imitating the corrosion mechanism. The modeling approaches of corrosion have presented in 3-dimensional transient times in CFD simulation. Surface reactions were performed by Species Model which involve site species. Site species in Species Model took place at gas-solid interfaces and in this case are salt vapor and surface pipe. Chemical reaction rate on the surface controls lost weight of a welded pipe and the model can be validated with experiment. In conclusion, in period 0-600 hours error between CFD modeling and experiment have error trend decreased. The error at 600 hours is 6% both of vertical pipe and horizontal pipe test. The modeling approaches closely with the performed experiment and can be accepted. Moreover, the model is able to predict corrosion of a welded pipe of different sizes and their lost weight after 600 hours without experiment. Also the model can predict lifetime of pipe.

Keywords: Stainless Steel ASTM A312 Grade 304L; Under Salt Vapor; Corrosion Rate; Welding Procedure Specification; CFD Modeling

1. Introduction

Corrosion is the deterioration of a metal, which treasured metal were changed for the worse by metal transformed to the well-known compound 'the rust'. This process directiy affects the strength of metal directly, the rust area gave reduce in strength [1-3]. The usage of steel pipes Wireless is new because of various properties of materials such as the mechanical and physical properties that are resistant to corrosion, even in water or a solution containing a dilute acid, when compare with steel. Generally, it was found that the steel is corrosion-prone with atmospheric moisture [4]. A stainless steel band Ostend forensics is a group with the use of large quantities of usable ranges. Low temperatures and high formability are easier to provide high strength, the main key is to

Preprints (www.preprints.org) | NOT PEER-REVIEWED | Posted: 12 December 2018 doi:10.20944/preprints201812.0144.v1

generate a thin film on the surface, called "film" to prevent corrosion for assembly [5]. Various types of stainless steel required heat and wire using to hold the pieces together. Moreover, it should use 'TIG' welding, a tungsten inert gas welding, to produce covered gas because the welding process to melt into highly usable spacious and save money. However, a common problem after welding is the only intergranular corrosion in the summer. Heat affected zone (HAZ) of stainless steel caused heat accumulated after welding of stainless steel was gradually cooled over the critical temperature. The chromium moved to combine with carbon compounds and formed to be chromium carbide ($Cr_{23}C_6$) [6-11]., and then precipitated at the grain boundaries [7-9] made of stainless steel, loss of corrosion resistance of welding in the so-called "link rot" [12] by stainless steel group, Austen's laws are inclined to corrosion. Many factors are influencing the initiation of one or several corrosion processes [13]. These factors include the nature of the material, surface finish, temperature, humidity, wind directions, rainfall, etc. To deal with the seawater corrosion, they are currently being developed with the aim to reduce corrosion, thus the corrosion mechanisms of these alloys must be determined. Generally [14], the corrosion testing is performed using salt-water by immersion, but it could not have simulated the real usage condition. Therefore, the salt-spray technique was used to verify according to ASTM B-117 [15]. Once in the grain boundary critical temperature range at 500-850 °C[16-18],of stainless steel was placed in a condition called "Sensitized", which caused the condition. Sensitization will be more or less dependent on the cooling temperature, time and chemical compounds [19]. Stainless steel is generally stainless-steel grade ASTM 304L with chrome create. Ostia Natick is currently very popular due to the strength and corrosion resistance, corrosive-wear or fretting-corrosion [20-22]. However, the deterioration of the environmental conditions surrounded by the atmosphere inside the casing, or the atmosphere of ice and salt to use part of the main factors that can be seen is corrosion damage both the look and structure of the physical erosion degraded the material cannot withstand. Corrosion is a material made of stainless steel are likely to be damaged by corrosion due to the strongly acidic environment [23-26], especially the surface of the material shown in Figure 1.

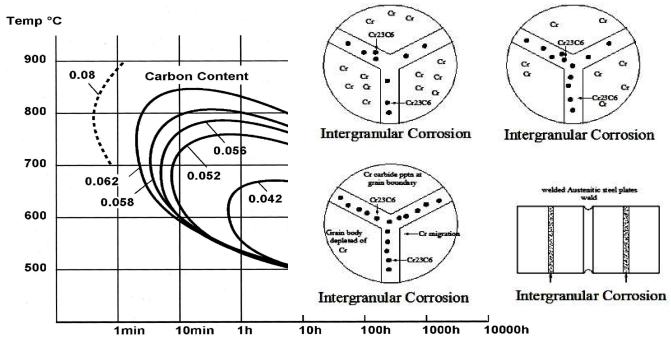

Figure 1 Shows a weld decay and precipitation of chromium carbide of austenitic stainless steel group [7].

Based on a review of CFD modeling corrosion, erosion–corrosion phenomena in pipe bend and CFD Modeling approximate quantity of the wall pipe. The erosion–corrosion phenomena in the pipe have four-phase flow comprise of two immiscible liquids, gas and particulate solid. A CFD tool has simulation the particle trajectories and impact rates inside the pipe. The Corrosion of metallic material has been considered. Erosion model parameters have been derived from experiments correlating particle impact angle and erosion rate. Corrosion model parameters have been obtained from electrochemical measurements. The modeling operating parameters comprise of fluid flow velocity, particulate content and gas volume fraction. The modeling has been evaluated by a two-state in experiments approach. The first state effects on synergistic damaging and the ratio of corrosive to overall damaging have been identified. The second state is erosion-enhanced and erosion-limited effects of flow conditions have been highlighted for the passivating and the actively corroding alloys by Benedetto Bozzini et al.[28]. CFD simulation of flow-assisted corrosion of

 doi:10.20944/preprints201812.0144.v1

aluminum alloy in ethylene glycol–water solution. The impingement jet system is a tool of study flow-assisted corrosion (FAC) of 3003 Aluminum (Al) alloy in ethylene glycol–water solutions. The modeling occurred in the automotive coolant. The corrosion potential and electrochemical impedance spectroscopy (EIS) measurements from the experiment. The solution and impact angle on Al FAC were measure from the experiment. The solution has increased to enhances the activity of Al due to the dissolution of Al oxide film in an alkaline environment. In the experiment, The activity of Al decreases with increasing fluid impact angle to the specimen. The Modeling shows the impact angle increase the electrode area under high-velocity flow field decreases and low-velocity flow field increases by L.Y.Xu et al.[29]. The modeling of erosion–corrosion of Fe in aqueous conditions from particle concentration. The model has been developed to explain the effects of particle concentration on the erosion–corrosion of the inner surfaces of a circular pipe of 90° bend at room temperatures. The results show that the corrosion-dominated regime at the pipe bend is reduced with an increase in particle concentration by M.M.Stack et al.[30].

This paper presented 3-dimensional (3D) corrosion of a welded stainless-steel pipe under salt vapor condition. In this experiment, the weight of a welded pipe has been lost because of corrosion. A welded pipe is a stainless-steel ASTM A312 grade 304L and period of an experiment about 600 hours that they are tested in vertical and horizontal alignments. The current of welding has set at 60 A, 70 A to 80 A for showing the effect of current with corrosion. A lost weight of a welded pipe evaluates by CFD modeling. In CFD software, there is not directly model of corrosion, but it can use surface reaction technique to corrosion model. The key of corrosion phenomenon is a surface reaction on the wall of a welded pipe. In order to create modeling approach lost weight of a welded pipe for estimate lost weight and corrosion prediction in difference size without experiment cost. CFD software can be performed by Species Model in ANSYS FLUENT software. Results of validation in period 0-600 hours can be used represents corrosion phenomena in a welded pipe. The modeling leads to predicting the effect of a different size and lost weight after 600 hours.

2. Model Description

In corrosion of a welded stainless-steel pipe under salt vapor condition, modeling can be represented by setting condition as same as experiment. The salt vapor injection flow can be performed by the laminar flow. The energy equation is used for the reaction. The species model is used for setting surface reaction. In species model, wall surface reactions and chemical vapor deposition is used for reaction in the model. Mass deposition source is used because the loss of mass due to surface that model is not mass balance. In options, the diffusion energy source is used for the effect of enthalpy transport due to species diffusion in the energy equation. The full multicomponent diffusion is used for activates Stefan-Maxwell's equations and computes the diffusive fluxes of all species in the mixture to all concentration gradient. The turbulence-chemistry interaction uses laminar finite-rate for this model.

2.1. Laminar flow of salt vapor flow

The laminar flow used in the model to represent salt vapor flow in control volume. The momentum equations for laminar flow in an inertial (non-accelerating) reference frame are given by

$$\frac{\partial}{\partial t}(\rho\vec{v}) + \nabla\cdot(\rho\vec{v}\vec{v}) = -\nabla p + \nabla\cdot\left(\bar{\bar{\tau}}\right) + \rho\vec{g} + \vec{F} \tag{1}$$

where p is the static pressure, $\bar{\bar{\tau}}$ is the stress tensor, $\rho\vec{g}$ and $\vec{F}$ are the gravitational body force and external body forces, respectively.

The stress tensor $\bar{\bar{\tau}}$ is given by: $\bar{\bar{\tau}} = \mu\left[\left(\nabla\vec{v} + \nabla\vec{v}^{T}\right) - \frac{2}{3}\nabla\cdot\vec{v}I\right]$ (2)

where μ is the molecular viscosity, I is the unit tensor, and the second term on the right-hand side is the effect of volume dilation.

2.2. Energy equation of reaction in the model

 doi:10.20944/preprints201812.0144.v1

The reaction in model considers enthalpy of reaction. The energy equation is enabled to considering enthalpy of reaction. The enthalpy of the material is computed as the sum of the sensible enthalpy, h, and the latent heat, ΔH:

where $$H = h + \Delta H \tag{3}$$

$$h = h_{ref} + \int_{T_{ref}}^{T} c_p dT \tag{4}$$

and h_{ref} = reference enthalpy, T_{ref} = reference temperature, c_p = specific heat at constant pressure

2.3. Wall surface reactions and chemical vapor deposition of reaction in the model

The phenomena of a welded pipe are corrosion. The corrosion is a chemical reaction which is occurred at the surface of the pipe. It can be represented corrosion by wall surface reactions and chemical vapor deposition in a species model. Consider the r th wall surface reaction written in general form as follows:

$$\sum_{i=1}^{Ng} g_{i,r}^{'} G_i + \sum_{i=1}^{Nb} b_{i,r}^{'} B_i + \sum_{i=1}^{Ns} s_{i,r}^{'} S_i \xrightarrow{K_r} \sum_{i=1}^{Ng} g_{i,r}^{''} G_i + \sum_{i=1}^{Nb} b_{i,r}^{''} B_i + \sum_{i=1}^{Ns} s_{i,r}^{''} S_i \tag{5}$$

where G_i, B_i, and S_i represent the gas phase species, the bulk (or solid) species, and the surface-adsorbed (or site) species, respectively. N_g, N_b, and N_s are the total numbers of these species. $g_{i,r}^{'}$, $b_{i,r}^{'}$, and $s_{i,r}^{'}$ are the stoichiometric coefficients for each reactant species i, $g_{i,r}^{''}$, $b_{i,r}^{''}$, and $s_{i,r}^{''}$ are the stoichiometric coefficients for each product species i. The K_r is the overall constant rate of reaction.

The summations in Equation (5) are for all chemical species in the system, but only species involved as reactants or products will have non-zero stoichiometric coefficients. Hence, species that are not involved will drop out of the equation.

The rate of the r reaction is $$R_r = k_{f,r} \prod_{i=1}^{Ng} [G_i]_{wall}^{g_{i,r}^{'}} [S_i]_{wall}^{s_{i,r}^{'}} \tag{6}$$

where $[\ ]_{wall}$ represents molar concentrations on the wall. It is assumed that the reaction rate does not depend on concentrations of the bulk (solid) species. From this, the net molar rate of production or consumption of each species i is given by

$$\hat{R}_{i,gas} = \sum_{r=1}^{N_{rxn}} \left(g_{i,r}^{''} - g_{i,r}^{'} \right) R_r \qquad i = 1,2,3,...,N_g \tag{7}$$

$$\hat{R}_{i,\text{bulk}} = \sum_{r=1}^{N_{rxn}} \left(b_{i,r}^{''} - b_{i,r}^{'} \right) R_r \qquad i = 1,2,3,...,N_b \tag{8}$$

$$\hat{R}_{i,\text{site}} = \sum_{r=1}^{N_{rxn}} \left(s_{i,r}^{''} - s_{i,r}^{'} \right) R_r \qquad i = 1,2,3,...,N_s \tag{9}$$

The forward rate constant for the reaction $r\left(k_{f,r}\right)$ is computed using the Arrhenius expression:

$$k_{f,r} = A_r T^{\beta r} e^{-E_r / RT} \tag{10}$$

where A_r = pre-exponential factor (consistent units)

β_r = temperature exponent (dimensionless)

E_r = activation energy for the reaction $\left(j / kgmol\right)$

R = universal gas constant $\left(j / kgmol \cdot K\right)$

2.4. The full multicomponent diffusion for diffusive fluxes in model.

A chemical species diffusion in the species transportations and energy equations are important when details of the molecular transport processes are significant. As one of the laminar-flow diffusion models, FLUENT can model full multicomponent species transport. The Maxwell-Stefan equations will be used to obtain the diffusive mass flux. This will lead to the definition of generalized Fick's law diffusion coefficients. This method is preferred over computing the

Preprints (www.preprints.org) | NOT PEER-REVIEWED | Posted: 12 December 2018 doi:10.20944/preprints201812.0144.v1

multicomponent diffusion coefficients since their evaluation requires the computation of N^2 co-factor determinants of size $(N-1)\times(N-1)$, and one determinant of size $N\times N$, when N is the number of chemical species. The Maxwell-Stefan equations can be written as:

$$\sum_{\substack{j=1\\ j\neq 1}}^{N}\frac{X_i X_j}{D_{ij}}\left(\vec{V}_j-\vec{V}_i\right)=\vec{d}_i-\frac{\nabla T}{T}\sum_{\substack{j=1\\ j\neq 1}}^{N}\frac{X_i X_j}{D_{ij}}\left(\frac{D_{T,j}}{\rho_j}-\frac{D_{T,i}}{\rho_i}\right) \tag{11}$$

where X is the mole fraction, $\vec{V}$ is the diffusion velocity, D_{ij} is the binary mass diffusion coefficient, and D_T is the thermal diffusion coefficient.

For an ideal gas, the Maxwell diffusion coefficients are equal to the binary diffusion coefficients. If the external force is assumed to be the same on all species and that pressure diffusion is negligible, then $\vec{d}_i=\nabla X_i$.

3. Experiment

3.1. Specimen preparation

The experimental materials used were ASTM A312 stainless steel pipe Grade 304L is a wireless pipe seam used to transport liquid hose system that require resistance to corrosion by stainless pipe size from (2.77 mm thick x 103 mm) was prepared from 304L stainless steel by gas tungsten arc welding process (GTAW).In ASTM Standards of stainless steel pipe obtaining from spectrometer is shown in Table 1. The chemical composition of the electrode ER 308L solid electrodes used in this study obtaining from spectrometer is shown in Table 2.

Table1. Chemical compositions of the ASTM A312 stainless steel pipe Grade 304L by spectrometer.

Atomic Percentage (%)									
C	Mn	P	S	Si	Cr	Cu	Mo	Ni	Fe
0.08	2.00	0.040	0.03	0.75	18.0 - 20.0	-	0.082	8.0 - 11.0	Bal.

Table 2. Chemical compositions of the solid electrode by spectrometer [31].

AWS Classification	Atomic Percentage (%)									
AWS A 5.9	C	Mn	Si	P	S	Ni	Cr	Mo	V	Cu
ER 308L	0.03	1.5	0.50	0.50	0.03	10	19.5	0.75	-	0.75

For the welding, the welding procedure specifications (WPS) for the piping specimens was used to weld all the piping specimens and was based on the ASME Section IX 2015 [32]. To ensure that the WPS produced a good weld, the welded specimens obtained from various welding currents were tested for the ultimate tensile (according to the ASME Section IX 2015) and infiltration (ASME Section V article 6) to make the procedure qualification record (PQR). The piping specimens were welded using the tungsten arc welding gas (GTAW) technique [33]. The welding currents used in the study were 60 A (heating values of welding 0.90 kJ/mm), 70 A (heating values of welding 0.95 kJ/mm) and 80 A (heating values of welding 1.02 kJ/mm) [34].

3.2. Salt Spray Test

The test procedure with the salt spray test with Salt mist is the process by bringing the target test in the chamber that is used to test that the design and the control to the apparatus, of ASTM D B117. By using the Solution salt concentration is 5%, which prepared by the melt the Sodium Chloride (NaCl) in the water was touched to standard D1193 ASTM.specification for coolants, type lV and to have a system to flow into the internal chamber it will have to adjust the condition within the prior to the actual test before using the internal temperature around 35 degrees Celsius and spray salt 5% rate with 12 milliliters per hour. There will be a buildup of the salt spray in rate of at

Preprints (www.preprints.org) | NOT PEER-REVIEWED | Posted: 12 December 2018 doi:10.20944/preprints201812.0144.v1

least 80 cubic centimeters of Graduated within the cylinder chamber first will keep it near the spray the salt and again the cylinder from the syringe as shown in Figure 2

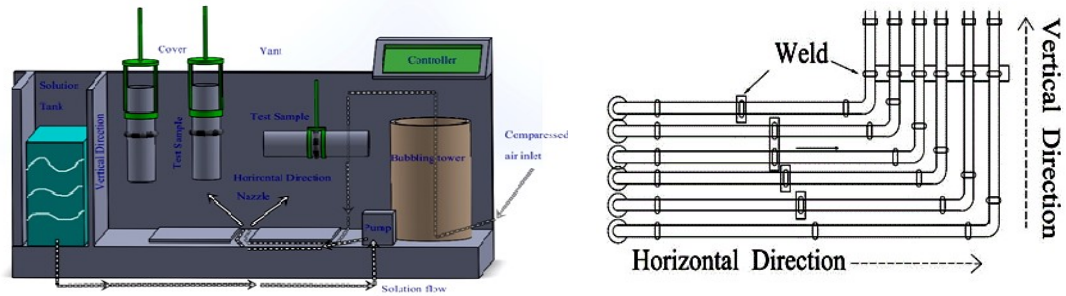

(a) (b)

Figure 2. The test with Salt mist that supports the ASTM D B117: (a) Salt spray Tester and (b) Direction of testing specimens.

3.3. Characterization and Equipment

3.3.1. Material Verification

According to WPS for ASTM A312 stainless steel pipe Grade 304L welded pipe, a weld connection of a 103 mm distance was used as a welded piping specimen as shown in Figure 4a. Following the penetrant testing procedure, the surfaces of the specimens were cleaned. The work-piece was sprayed, covering all over the specimen, and left for 10 min for opening the surface penetrant. After that, the specimens were wiped down to remove excess penetrant and then wiped with a cleaning solution again to ensure that the excess penetrant near the weld area was remove

Standard equipment Penetrant testing (PT) for MIL-I-25135[33], The welded pipes obtained from welding currents at 60, 70 and 80 A were inspected by radiographic testing with the X-ray source for AWS D1.1 Standard [34], and Emission Spectrometer for Salt Spray Test ASTM D B117.

4. Simulation, Results and Discussion

4.1. Model and boundary condition

4.1.1. Reaction of model

The modeling surface reaction in model is used like a desorption reaction. The desorption reaction can explain by wall has reaction with some species after some of wall spit out with species as well. Basically, surface reaction in welded pipe is iron oxide also known as rust because stainless-steel has compound with iron. In create desorption reaction of welded pipe, iron of welded pipe has spit out from wall of welded pipe follows the chemical reaction:

$$4Fe^{2+} + O_2 \rightarrow 4Fe^{3+} + 2O^{2-} \quad (12)$$

Reaction (12) also known as redox reaction that oxidation of iron compound with oxygen

$$Fe^{2+} + 2H_2O \rightarrow Fe(OH)_2 + 2H^+ \quad (13)$$

$$Fe^{3+} + 3H_2O \rightarrow Fe(OH)_3 + 3H^+ \quad (14)$$

Reaction (13) and (14) is oxidation of iron compound with water In experiment, salt vapor injects in control volume 12 milliliters per hour. The salt vapor is solution which salt has concentration is 5% that mean water is 95% for injection. The water became effect to oxidation of iron rather than salt. In model, water is used create desorption reaction:

$$2H_2O + Fe\_s \rightarrow Fe^{2+} + 2(OH) + Fe^{2+}\_s + 2H \quad (15)$$

where Fe_s is surface of welded pipe.

Fe^{2+} is oxidation of iron that spit out from surface of welded pipe.

Fe^{2+}_s is add-on surface of welded pipe for balance site species and represent surface after oxidation of iron is gone.

Preprints (www.preprints.org) | NOT PEER-REVIEWED | Posted: 12 December 2018 doi:10.20944/preprints201812.0144.v1

In reaction (15) is built in model, reaction is occurred before equation (13) that oxidation of iron form with $2(OH)$.In the meantime, reaction (15) make Fe^{2+}_s at surface of welded pipe in model that it makes surface of pipe can't react with H_2O in model again. The problem can be solved by make chemical reaction to convert Fe^{2+}_s to Fe_s for model can continuously operate desorption reaction. The chemical reaction is:

$$2H_2O^+ + Fe^{2+}\_s \rightarrow Fe\_s + 2H_2O \quad (16)$$

where H_2O^+ is add-on species for convert surface to Fe_s

Table 3. Reaction Parameters of Desorption Reaction in Model.

Parameter	**For Reaction (15)**	**For Reaction (16)**
Reaction Type	Wall Surface	Wall Surface
Number of Reactant	2	2
Species	H_2O , Fe_s	H_2O^+ , Fe^{2+}_s
Stoichiometry Coefficient	H_2O =2, Fe_s =1	H_2O^+ =2, Fe^{2+}_s =1
Rate Exponent	H_2O =2, Fe_s =1	H_2O^+ =2, Fe^{2+}_s =1
Number of Product	4	2
Species	Fe^{2+} , Fe^{2+}_s , (OH) , H	Fe_s , H_2O
Stoichiometry Coefficient	Fe^{2+} =1, Fe^{2+}_s =1, (OH) =2, H =2	Fe_s =1, H_2O =2
Rate Exponent	Fe^{2+} =0, Fe^{2+}_s =0, (OH) =0, H =0	Fe_s =0, H_2O =0
For Vertical Pipe		
Pre-Exponential Factor = PEF	1.1×10^{-7}	1.1×10^{-7}
Activation Energy = AE	0	0
Temperature Exponent = TE	0	0
For Horizontal Pipe		
Pre-Exponential Factor = PEF	1.1×10^{-7}	1.3×10^{-7}
Activation Energy = AE	0	0
Temperature Exponent = TE	0	0

The reaction mechanisms set wall surface of reaction type both reactions. The site density is 10^{-8}[kgmol/ m2] .The site parameters of reaction (15) and (16) are Fe_s and Fe^{2+}_s that initial site coverage are 0.5 both of species.

4.1.2. Species of model

The specie properties of chemical reaction (15) and (16) are adapted to explained corrosion. The add-on species is not real species but they are used for surface in model like real surface of pipe. Therefore, some of the specie properties is not real. The specie properties shown in table 4

Table 4. property of species in model.

Chemical Formula	H_2O	H_2O^+	(OH)	H	Fe^{2+}	Fe_s	Fe^{2+}_s
Density	incompressible-ideal-gas	incompressible-ideal-gas	incompressible-ideal-gas	incompressible-ideal-gas	incompressible-ideal-gas	incompressible-ideal-gas	incompressible-ideal-gas
Cp	kinetic-theory	kinetic-theory	kinetic-theory	kinetic-theory	kinetic-theory	kinetic-theory	kinetic-theory
Thermal Conductivity	kinetic-theory	kinetic-theory	kinetic-theory	kinetic-theory	kinetic-theory	kinetic-theory	kinetic-theory
Viscosity	kinetic-theory	kinetic-theory	kinetic-theory	kinetic-theory	kinetic-theory	kinetic-theory	kinetic-theory
Molecular Weight	18	19	17	1	1	55.845	54.845
Standard State Enthalpy	0	0	0	0	0	0	0
Standard State Entropy	0	0	0	0	0	0	0

Preprints (www.preprints.org) | NOT PEER-REVIEWED | Posted: 12 December 2018 doi:10.20944/preprints201812.0144.v1

Reference Temperature	298.15	298.15	298.15	298.15	298.15	298.15	298.15
Degrees of Freedom	0	0	0	0	0	0	0

4.1.3. Inlet boundary condition of model

The salt vapor injects in salt spray tester 12 milliliters per hour. that is inlet in boundary condition. The salt vapor is solution also known as chloralkali process salt concentration is 5% of 12 milliliters per hour. The chemical reaction of salt vapor is:

$$2NaCl(5\%) + 2H_2O(95\%) \rightarrow [Cl_2 + H_2 + 2NaOH](5\%) + 2H_2O(95\%) \quad (17)$$

according chemical reaction, spray $H_2O(95\%)$ and $[Cl_2 + H_2 + 2NaOH](5\%)$ of 12 milliliters per hour into inlet boundary condition. The mole fraction of species follows chemical reaction (17) have setting up in mass flow inlet type. The chemical reaction show H_2O has effect to surface of pipe rather than species other that is explained in reaction of model. The species in mass flow inlet are used mole fraction. The mole fraction of H_2O and H_2O^+ are 0.5.

4.1.4. Salt Spray Test Results

The continuous spray application for 200 - 600 hours was carried out in the experimental study. The duct area was not significantly different from the conventional one. The weld area is rusted as shown in Figure 3

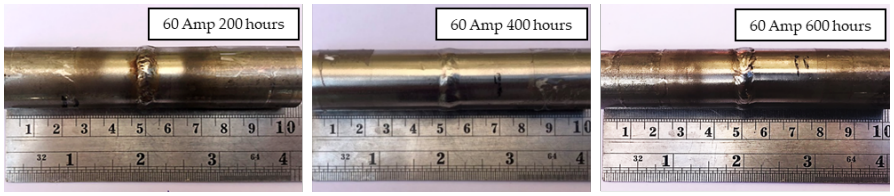

Figure 3. Vertical pipe characteristics at welding currents 60 A tested with salt spray at 200 400 and 600 h.

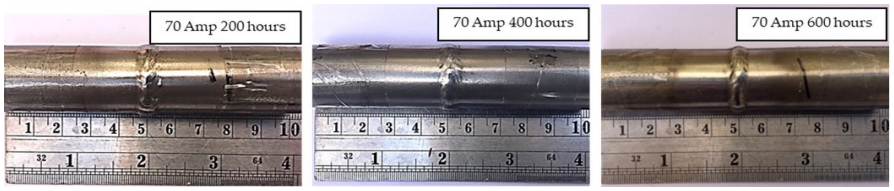

Figure 4 Vertical pipe characteristics at welding current 70 A tested with salt spray at 200 400 and 600h.

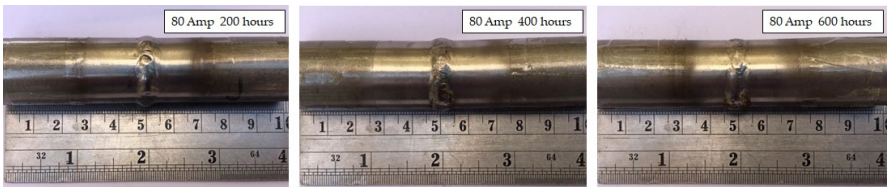

Figure 5 Vertical pipe characteristics at welding current 80 A tested with salt spray at 200 400 and 600h.

 doi:10.20944/preprints201812.0144.v1

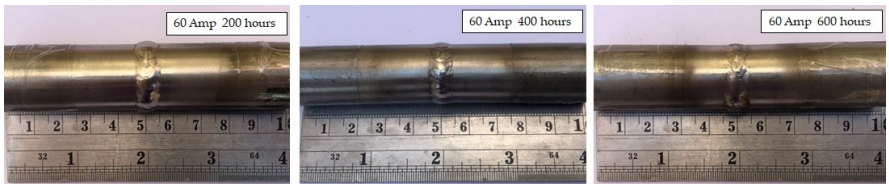

Figure 6 Horizontal pipe characteristics at welding currents 60 A tested with salt spray at 200 400 and 600h.

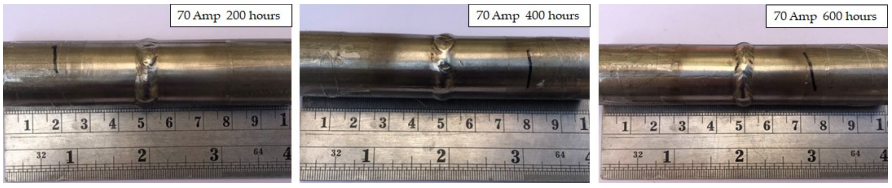

Figure 7 Horizontal pipe characteristics at welding current 70 A tested with salt spray at 200 400 and 600h.

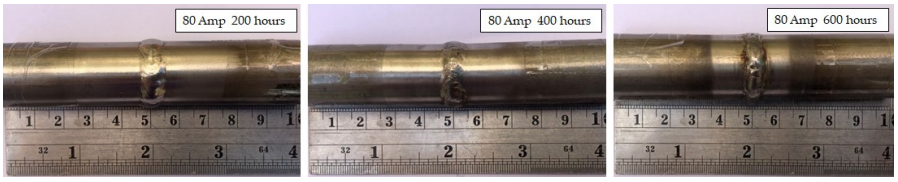

Figure 8 Horizontal pipe characteristics at welding currents 80 A tested with salt spray at 200 400 and 600h.

Based on the weight data of the pipeline before and after the test with vapor, it was found that the test tube had a higher weight. Since the weld is corrosive, the iron (Fe) of the pipe element changes to high iron oxide (Fe_2O_3) or rust, so it is possible to determine the corrosion effect of the pipe from the change in pipe weight data (Relative Weight as shown in Table 6 and the corrosion rate can be calculated as shown in Table 5-7.

Table 5 Shows the weight of the welded pipe before testing with salt vapor.

60 amperes			
Piece	**Vertical (g)**	**Piece**	**Horizontal (g)**
1	124.396	1	123.181
2	122.470	2	123.217
3	123.695	3	122.520
70 amperes			
Piece	**Vertical (g)**	**Piece**	**Horizontal (g)**
1	121.873	1	120.134
2	121.889	2	121.665
3	122.318	3	122.314
80 amperes			
Piece	**Vertical (g)**	**Piece**	**Horizontal (g)**
1	121.378	1	121.666
2	124.558	2	121.929
3	120.633	3	122.357

Preprints (www.preprints.org) | NOT PEER-REVIEWED | Posted: 12 December 2018 doi:10.20944/preprints201812.0144.v1

Table 6 Shows the weight of the hose tested.

Specimens / Time (h)	Weight			Relative Weight		
	200 h	400 h	600 h	200 h	400 h	600 h
V60 A	0.025	0.036	0.041	0.00015	0.00029	0.00033
V70 A	0.031	0.042	0.043	0.00025	0.00030	0.00035
V80 A	0.023	0.036	0.036	0.00014	0.00027	0.00031
H60 A	0.042	0.059	0.058	0.00020	0.00034	0.00035
H70 A	0.030	0.038	0.035	0.00023	0.00025	0.00029
H80 A	0.028	0.037	0.040	0.00020	0.00023	0.00033

Table 7 Shows the corrosion rates of test tubes with salt vapor.

Specimens / Time (h)	(Corrosion rate) mm/year			K constant
	200 h	400 h	600 h	slope
V60 A	0.032	0.023	0.017	2.000
V70 A	0.039	0.027	0.018	2.003
V80 A	0.029	0.023	0.015	1.999
H60 A	0.053	0.037	0.025	2.005
H70 A	0.038	0.024	0.020	2.005
H80 A	0.036	0.023	0.017	2.001

From the test results with steam, the steam found in the salt vapor at a greater time. The increase in weight due to rust is shown in Table 7 And the corrosion rate found that the welded pipe at 80 ampere has the lowest corrosion rate of 0.017 millimeters per year. Considering the slope value. The slope of the corrosion graph shows that the vertical workpiece has a lower erosion rate than the horizontal workpiece, as shown in Figures 9 and Figures 10.

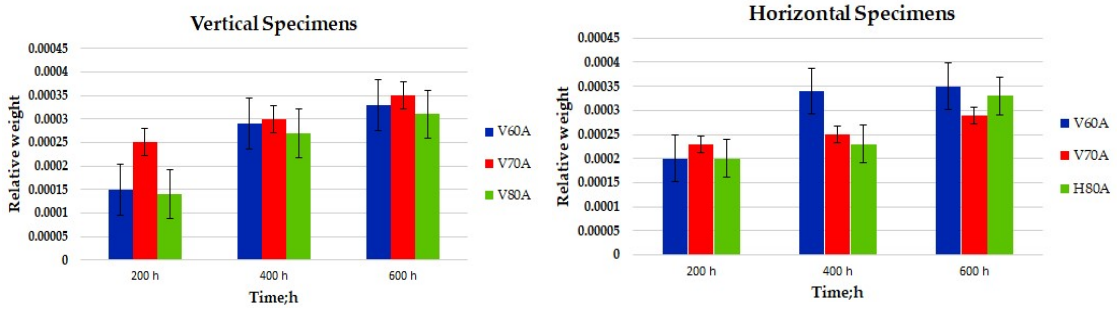

Figure 9 Graph of pipe weight and time to be tested with salt vapor.

Preprints (www.preprints.org) | NOT PEER-REVIEWED | Posted: 12 December 2018 doi:10.20944/preprints201812.0144.v1

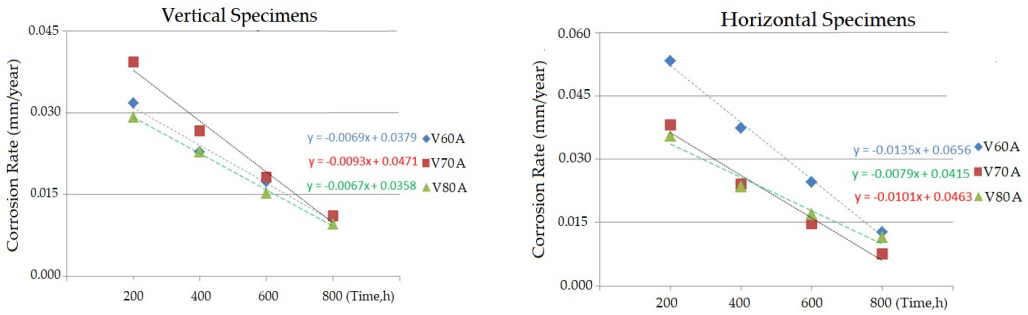

Figure 10 Graph plot showing the corrosion rate of 304 stainless steel pipe welded at various currents.

4.2. Results and discussion of simulation

4.2.1. Species of oxidation of iron in model

The species of oxidation iron in CFD modeling can explained the corrosion of pipe. Moreover, it can explain area that is high or low corrosion in each alignment at 200 hours, 400 hours, and 600 hours. In figure, red color of area is explained that corrosion rate is high and blue color of area is explained corrosion rate is low and can be shows the effect of pipe alignment. Shown in figure 11 and 12.

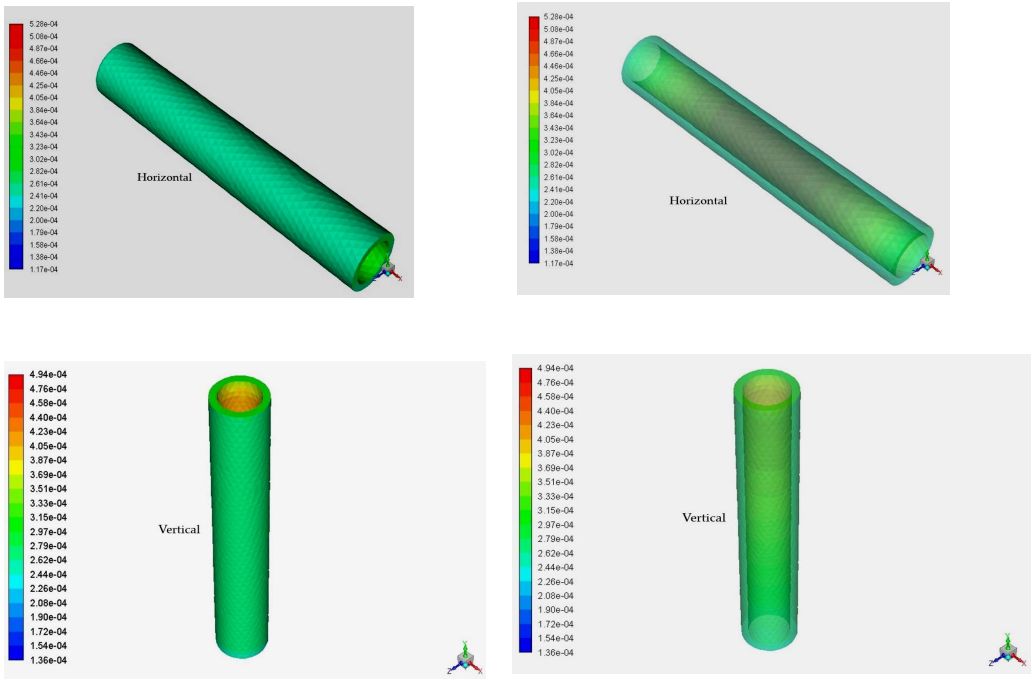

Figure 11 Mass fraction of oxidation iron species both of outside and inside pipe in horizontal and vertical pipe test at 200 hours.

Preprints (www.preprints.org) | NOT PEER-REVIEWED | Posted: 12 December 2018 doi:10.20944/preprints201812.0144.v1

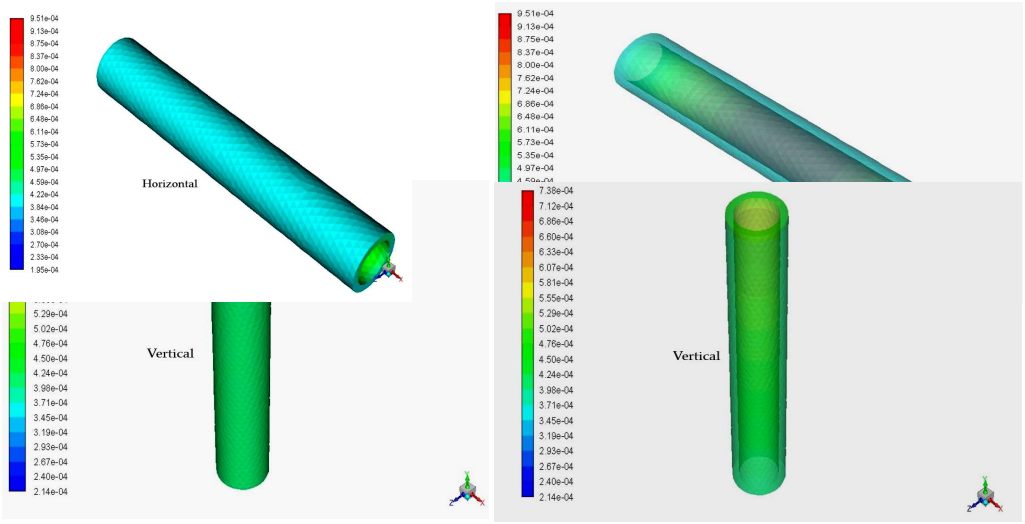

Figure 12 Mass fraction of oxidation iron species both of outside and inside pipe in horizontal and vertical pipe test at 400 hours.

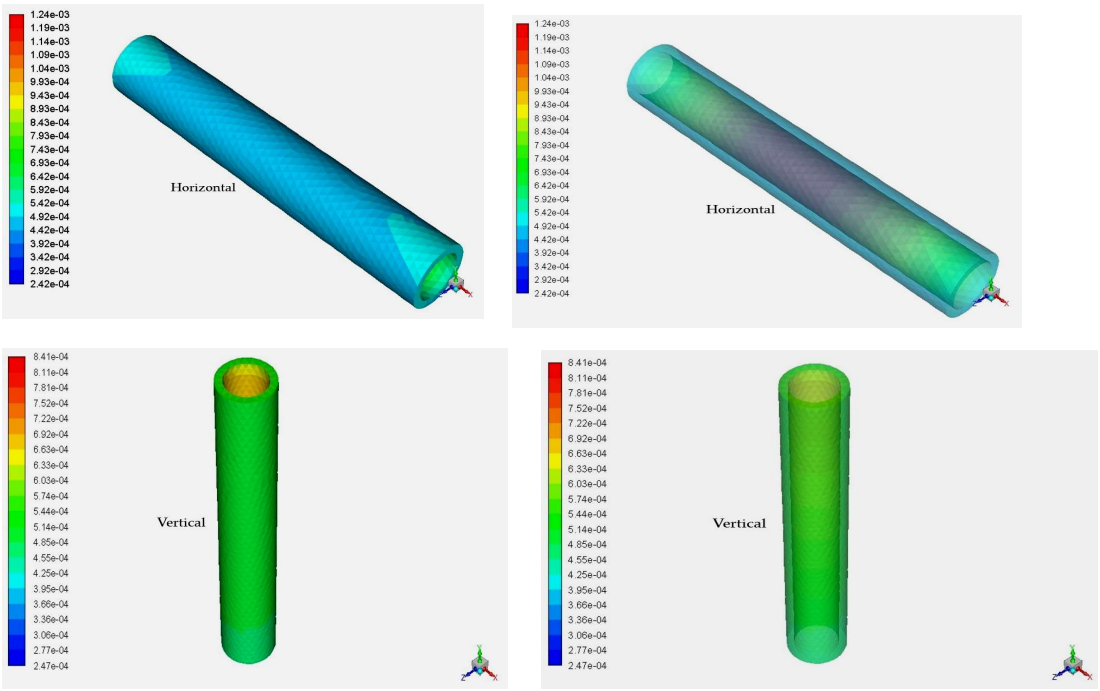

Figure 13 Mass fraction of oxidation iron species both of outside and inside pipe in horizontal and vertical pipe test at 600 hours.

The mass fraction of oxidation iron in figure (11)-(13) are mass oxidation iron of mass total that not mean mass lost in surface. The mass lost is used validation in 4.3.2 that is mass integral of control volume. The mass fraction of oxidation iron in figure use show area that they have different corrosion rate from effect of alignment.

4.2.2. lost weight validation

In lost weight validation, the CFD model represent by blue line and other line is experiment which are current welding at 60 A, 70 A and 80 A shown in figure 14 and 21. At 200 hours, lost weight is not nearly both of experiment and CFD modeling, maximum error between CFD modeling

Preprints (www.preprints.org) | NOT PEER-REVIEWED | Posted: 12 December 2018 doi:10.20944/preprints201812.0144.v1

and experiment, vertical pipe test is 32% at current of 70 A and horizontal pipe test is 26.52% at current of 70 A. At 400 hours, lost weight is closely both of experiment and CFD modeling, maximum error between CFD modeling and experiment is 7.33% at current of 70 A for vertical pipe test but horizontal pipe test is not closely error is 20.29% at current 60. At 600 hours, lost weight is closely both of experiment and CFD modeling, maximum error between CFD modeling and experiment, vertical pipe test is 6% at current of 70 A and horizontal pipe test is 6% at current of 70 A. The error trend is decrease both of vertical pipe test and horizontal pipe test. The lost weight validation of CFD Modeling can be accepted in period 0-600 hours.

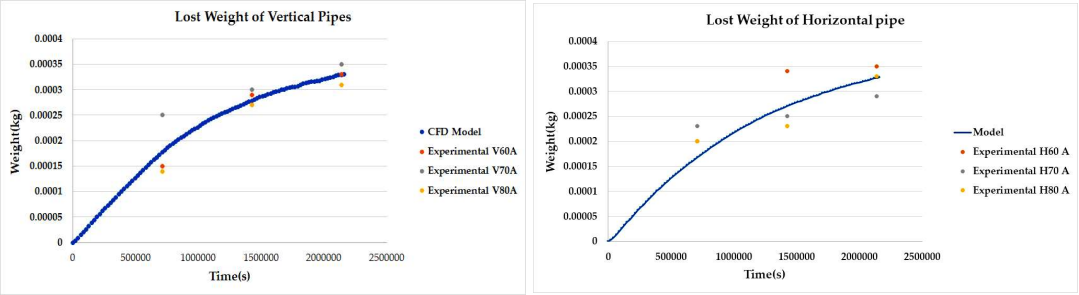

Figure 14 Graph compare lost weight between CFD modeling and welded pipes at three current for vertical and horizontal alignment.

5. Conclusions

In this study, both experiment and simulation work have been performed in order to understand corrosion mechanism. The experiment is given result but can't understand corrosion mechanism. The simulation work is used to mathematically explain corrosion mechanism which is same result of experiment. In CFD software, there is not directly model of corrosion but it can use surface reaction and create add-on chemical reaction technique for explain corrosion mechanism. The validation uses lost weight from experiment and CFD modeling at 200 hours, 400 hours, and 600 hours. A welded pipe is a stainless-steel ASTM A312 grade 304L and period of experiment about 0-600 hours that they are tested in vertical and horizontal alignments. In simulation, the salt vapor injection flow can be performed by is laminar flow. The energy equation is used for reaction. The species model is used for wall surface reactions and chemical vapor deposition. Mass deposition source is used because loss of mass due to surface that model is not mass balance. The diffusion energy source is used for effect of enthalpy transport. The full multicomponent diffusion is used for activates Stefan-Maxwell's equations. The modeling surface reaction in model is used like a desorption reaction. The desorption reaction has created and add-on species and chemical reaction for imitation corrosion pipe mechanism by reaction (15) and (16). The result of validation at 200 hours, lost weight is not nearly both of experiment and CFD modeling, maximum error between CFD modeling and experiment, vertical pipe test is 32% at current 70 A and horizontal pipe test is 26.52% at current 70 A. At 400 hours, lost weight is closely both of experiment and CFD modeling, maximum error between CFD modeling and experiment is 7.33% at current of 70 A for vertical pipe test but horizontal pipe test is not closely and error is 20.29% at current 60. At 600 hours, lost weight is close both of experiment and CFD modeling, with maximum error between CFD modeling and experiment, vertical pipe test is 6% at current of 70 A and horizontal pipe test 6% at current of of 70 A. The error trend decreases both of vertical pipe test and horizontal pipe test. The CFD Modeling lost weight validation can be accepted in period 0-600 hours.

Acknowledgments: The authors would like to acknowledge the Kasetsart University and Development Institute (KURDI).

Author Contributions: T. Yingsamphanchareon and A. Rodchanarowan performed this reseach

Conflicts of Interest: The authors declare no conflict of interest.

 doi:10.20944/preprints201812.0144.v1

References

[1] American Society for Testing and Materials. Standard Specification for Seamless Carbon Steel Pipe for High-Temperature Service. West Conshohocken.

[2] 2. H. A. E1-Dahan, T. Y. Soror, R. M. El-Sherif., Mater. Chem.Phys. 89 (2005) 260.

[3] S. A. Ali, M. T. Saeed, S. V. Rahman, Corros. Sci., 45 (2003) 253

[4] W. H. J. Vernon and L. Whitby; J. Inst. Metals, 44 (1930) 389.

[5] ASME Boiler and Pressure Vessel Committee, 2006, Section V, Nondestructive Examination, The American Society of Mechanical Engineer, Newyork, USA, pp.105 - 118.

[6] Sindo Kou.,2002, Welding Metallurgy, 2nd, A John Wiley & Son, Inc., Publication, pp. 53-57, 122-136, 321-329, 396-424

[7] Zumelzu E., Sepulveda J. and Ibarra M. "Influence of micro-structure on the mechanical behavior of welded 316 L SS joints", J. Mater. Process. Technol., vol. 94, pp. 36-40, 1999.

[8] Yang S., Wang Z.J., Kokawa H. and Sato Y.S. "Grain boundary engineering of 304 austenitic stainless steel by laser surface melting and annealing", J. Mater. Sci., vol.42, pp. 847-853, 2007.

[9] William D., Jr. Callister, Materials, 2007, Science And Engineering: An Introduction, 7th edition, JohnWiley & Sons, USA., p.326.

[10] Dadfar M., Fathi M.H., Karimzadeh F., Dadfar M.R.and Saatchi A. "Effect of TIG welding on corrosion behavior of 316L stain-less steel", Mater. Lett., vol.61, pp 2343-2346, 2007.

[11] Lu B.T., Chen Z.K., Luo J.L., Patchett B.M., Xu Z.H., Pitting and stress corrosion cracking behavior in welded austenitic stainless steel, Electrochim. Acta., vol. 50, pp. 1391-1403, 2005.

[12] Moura V., Kina A.Y., Tavares S.S.M., Lima L.D. and Mainier F.B. "Influence of stabilization heat treatments on microstruc-ture, hardness and intergranular corrosion resistance of the AISI 321 stainless steel", J.Mater.Sci., vol.43, pp 536-540, 2008.

[13] D. Knotkova-Cermakova, J. Vickova and Kuchynka: werkst. Korros., 24 (1973) 684

[14] K. Barton; Schutz gegen atmospharische corrosion, Verlag Chemie, Weinheim (1972)

[15] ASTM B117-03, "Standard Practice for Operating Salt Spray Apparatus"(West Conshohocken, PA: ASTM International, 2003).

[16] Tuthill A.H. "Corrosion testing of austenitic stainless steel weld-ments", Weld. J, vol.5, pp.36-40. 2005.

[17] Sedriks A.J. "Corrosion of Stainless Steels", 2nd Edition, John Wiley & Sons,Inc., New York, 1996.

[18] White W.E.,"Observations of the influence of microstructure on corrosion of welded conventional and stainless steels", Mater. Charact., vol.28, pp. 349-358. 1992.

[19] P. V. Strekalov, V. V. Agatonov and Y.N. Mikhailovskii; Zasch. Met., 8 (1972) 577

[20] Taiwade RV, Patil AP, Ghugal RD, Patre SJ, Dayal RK. "Effect of welding passes on heat affected zone and tensile properties of AISI 304 stainless steel and chrome-manganese austenitic stainless steel." ISIJ Int 53, 102–9, 2013

[21] Huei-Sen Wang "Effect of Welding Variables on Cooling Rate and Pitting Corrosion Resistance in Super Duplex Stainless Weldments", Materials Transactions, Vol. 46, 2003, pp. 593-601

[22] Kou S. "Welding Metallurgy", 2nd Edition, New Jersey, pp. 431-446. 2003.

[23] J. R. Viche, F. E. Varela, G. Acuna, E. N. Condaro, B. M. Rosales, G. Moriena, A. Fernandez, Corros. Sci., 37 (1995) 941-961.

[24] J. R. Viche, F. E. Varela, E. N. Condaro, B. M. Rosales, G. Moriena, A. Fernandez, Corros. Sci., 39 (1997) 655-679.

 doi:10.20944/preprints201812.0144.v1

[25] F. Corvo, C. Haces, N. Betancourt, L. Maldonado, L. Veleva, M. Echevarria, O. T. de Rincon, A. Rincon, Corros. Sci. 39 (1997) 823-833.

[26] M. Morcillo, B. Chico, L. Mariaca, E. Otero, Mat. Perform, 38 (1999) 72-77.

[27] Zumelzu E., Sepulveda J. and Ibarra M. "Influence of micro-structure on the mechanical behavior of welded 316 L SS joints", J. Mater. Process. Technol., vol. 94, pp. 36-40, 1999.

[28] Bozzini, B., et al., Evaluation of erosion–corrosion in multiphase flow via CFD and experimental analysis. Wear, 2003. 255(1-6): p. 237-245.

[29] Xu, L. and Y. Cheng, Electrochemical characterization and CFD simulation of flow-assisted corrosion of aluminum alloy in ethylene glycol–water solution. Corrosion Science, 2008. 50(7): p. 2094-2100

[30]Stack, M. and S. Abdelrahman, A CFD model of particle concentration effects on erosion–corrosion of Fe in aqueous conditions. Wear, 2011. 273 (1): p. 38-42.

[31] Specification for Tungsten and Oxide Dispersed Tungsten Electrodes for Arc Welding and Cutting.Available online: http://sif.library.illinois.edu/bibframe/html/7654275.html (accessed on 15 August 2016).

[32] ASTM Sec.IX,2015 Boiler and Pressure Vessel Code An International : The American Society of Mechanical Engineers, Two Park Avenue New York,NY 10016 USA

[33] Subodh Kumar,A.S.Shahi."Effect of heat input on the microstructure and mechanical properties gas tungsten arc welded AISI 304 stainless steel joints'.Materials and design 32 (2011) 3617-3623

[34] Nowacki J, Rybicki P. "The influence of welding heat input on submerged arc welded duplex steel joints imperfections." *J Mater Process Technol* 164, 1082–8, 2005

[35] AWS D1 Committee on Structural Welding, 2006, Structural Welding Code-Steel: AWS D1.1/D1.1M:2006, American Welding Society, Miami, Florida, USA., p. 172.